Differences of Boreal Summer Intraseasonal Oscillations Simulated in an Atmosphere–Ocean Coupled Model and an Atmosphere-Only Model*

XIOUHUA FU

IPRC, SOEST, University of Hawaii at Manoa, Honolulu, Hawaii

BIN WANG

Department of Meteorology, and IPRC, SOEST, University of Hawaii at Manoa, Honolulu, Hawaii

(Manuscript received 30 June 2003, in final form 30 October 2003)

ABSTRACT

A series of small-perturbation experiments has been conducted to demonstrate that an atmosphere–ocean coupled model and an atmosphere-only model produce significantly different intensities of boreal summer intraseasonal oscillation (BSISO) and phase relationships between convection and underlying SST associated with BSISO. The coupled model not only simulates a stronger BSISO than the atmosphere-only model, but also generates a realistic phase relationship between intraseasonal convection and underlying SST. In the coupled model, positive (negative) SST fluctuations are highly correlated with more (less) precipitation with a time lead of 10 days as in the observations, suggesting that intraseasonal SST is a result of atmospheric convection, but at the same time, positively feeds back to increase the intensity of the convection. In the atmosphere-only model, however, SST is only a boundary forcing for the atmosphere. The intraseasonal convection in the atmosphere-only model is actually less correlated with underlying SST. The maximum correlation between convection and SST occurs when they are in phase with each other, which is in contrast to the observations. These results indicate that an atmosphere–ocean coupled model produces a more realistic ISO compared to an atmosphere-only model.

1. Introduction

The boreal summer intraseasonal oscillation (BSISO) is an important phenomenon that affects global weather and climate. It significantly regulates the onset and retreat of the Asian summer monsoons (Yasunari 1980; Wang and Xu 1997), tropical storm activity (Liebmann et al. 1994), even the subseasonal rainfall variability over North America (Mo 2000).

The BSISO is probably a result of interaction between mean Asian summer monsoon and the equatorial, eastward-moving Madden–Julian oscillation (MJO; e.g., Lau and Chan 1986; Chen et al. 1988; Lawrence and Webster 2002), which is primarily initiated and maintained by internal atmospheric dynamics. In fact, significant progress in understanding and simulating the BSISO and MJO has been achieved with a variety of stand-alone atmospheric models (Lau and Peng 1987; Wang 1988; Bladé and Hartmann 1993; Hu and Randall 1994; Wang and Xie 1997; Raymond 2001; among others). However, state-of-the-art atmospheric general circulation models (AGCMs) still strive to realistically simulate intraseasonal oscillations (Slingo et al. 1996; Waliser et al. 2003).

Observations from the Tropical Ocean Global Atmosphere Coupled Ocean–Atmosphere Response Experiment (TOGA COARE) experiments reveal coherent SST fluctuations associated with MJO in the western Pacific (Weller and Anderson 1996). The recent Bay of Bengal Monsoon Experiment (BOBMEX; Bhat et al. 2001) and Joint Air–Sea Monsoon Experiment (JASMINE; Webster et al. 2002) field campaigns also found significant SST fluctuations associated with BSISO in the Indian Ocean. The intraseasonal SST fluctuations have been shown to play a significant role in the simulations of MJO in theoretical (Flatau et al. 1997; Wang and Xie 1998) and numerical models (Waliser et al. 1999; Inness and Slingo 2003; Fu et al. 2003). Wu et al. (2002) found that the simulated MJO in AGCMs systematically leads the observations by a quarter of a cycle. Fu et al. (2003), by comparing a coupled run and an atmosphere-only run, showed that the BSISO in a

* School of Ocean and Earth Science and Technology Contribution Number 6292 and International Pacific Research Center Contribution Number 247.

Corresponding author address: Dr. Xiouhua Fu, IPRC, SOEST, University of Hawaii at Manoa, 1680 East–West Road, Post Bldg. 401, Honolulu, HI 96822.
E-mail: xfu@hawaii.edu

coupled run is about 50% stronger than that in the (Atmospheric Model Intercomparison Project) AMIP-type atmosphere-only run (with monthly mean SST as boundary forcing). Even forced with the daily mean SST from the coupled run, the BSISO in the atmosphere-only model is still 30% weaker than that in the coupled run. Furthermore, the phase relationships between the SST and convection associated with BSISO differ considerably between the coupled run and the atmosphere-only run. This result leads us to speculate that there could be different ISO solutions for a coupled model and for an atmosphere-only model. This hypothesis is examined in this paper.

2. Model and experiments

a. Model

The atmospheric component of this hybrid-coupled model is ECHAM4 AGCM, which was documented in detail by Roeckner et al. (1996). We used the T30 version with a horizontal resolution of about 3.75°. The model has 19 vertical levels extending from the surface to 10 hPa. The ocean component of this coupled model is a Wang–Li–Fu intermediate ocean model. It is a 2.5-layer tropical upper-ocean model, which was originally developed by Wang et al. (1995) and improved by Fu and Wang (2001) in the tropical Pacific. This ocean model is able to produce reasonable annual cycles of SST, upper-ocean currents, and mixed layer thickness in the tropical Pacific (Fu and Wang 2001). In the present study, the ocean model covers both tropical Indian and Pacific Oceans with realistic but simplified coastal boundaries. ECHAM4 AGCM has been successfully coupled with the Wang–Li–Fu ocean model without heat flux correction in the tropical Indian and western Pacific Oceans. This hybrid-coupled model reasonably simulates the mean Asian summer monsoon (Fu et al. 2002) and associated boreal summer intraseasonal oscillations (Fu et al. 2003). It also improves the simulation of the MJO compared to the stand-alone ECHAM4 AGCM (Kemball-Cook et al. 2002).

b. Experimental designs

In order to reveal the differences of ISO in the coupled model and atmosphere-only model, five experiments are carried out (Table 1). These experiments are designed to see how different the ISO will be between the coupled model and atmosphere-only model when a small amount of noise is introduced in the initial and/or boundary conditions. In order to keep the mean states close to each other in a coupled run and the corresponding atmosphere-only run, the SST outputs from the coupled runs have been used as boundary conditions of the atmosphere-only runs. There are two coupled runs and three atmosphere-only runs. The only difference between the two coupled runs is the choice of coupling procedure. In the directly coupled run (DCPL), the daily mean SST from the ocean model is *directly* passed to the atmospheric model. In the indirectly coupled run (ICPL), we saved daily mean SST from the ocean model first, and then passed the saved SST to the atmospheric component. *The saved SSTs were truncated.* The magnitude of truncation error is on the order of 0.002°C, which is much smaller than the uncertainties in current observational SST products. The DATM (Table 1) is an atmosphere-only run with the daily mean SST *saved* from the DCPL run as the lower boundary forcing. With respect to the atmospheric component, the only difference between the DATM run and the DCPL run is in SST truncation errors from the DATM run. The IATM (Table 1) is an atmosphere-only run forced with the saved daily mean SST from the ICPL run. In this case, the atmospheric components of the ICPL run and the IATM run have exactly the same initial or boundary conditions. Therefore, these two runs have identical BSISO solutions. To save space, the solution from the IATM run will not be shown in the following analysis. Another atmospheric run (IATMi; Table 1) is the same as the IATM except that the initial conditions have a 1-day difference. All five experiments were integrated for 10 yr. If the solutions of the coupled model differ from those of the atmosphere-only model, we should expect that 1) the group of DCPL and ICPL has similar BSISO solution; the group of DATM and IATMi has similar BSISO solution, but 2) the BSISO solutions of the two groups differ significantly.

3. Results

In the following analyses, we only focus on the boreal summer intraseasonal oscillations in the Indian sector.

TABLE 1. Sensitivity experiment conditions. (C) coupled run (with interactive ocean); (A) atmosphere-only run.

Labels	Initial condition	Boundary condition
DCPL(C)	ECMWF analysis at 1 Jan 1988	Direct coupling (save SST for the DATM)
DATM(A)	ECMWF analysis at 1 Jan 1988	Truncated SST from the DCPL
ICPL(C)	ECMWF analysis at 1 Jan 1988	Indirect coupling (Pass trucated SST to the atmosphere)
IATM(A/C)	ECMWF analysis at 1 Jan 1988	SST from the ICPL (SST is exactly the same as in the ICPL)
IATMi(A)	1-day difference from the ECMWF analysis at 1 Jan 1988	Same as the IATM

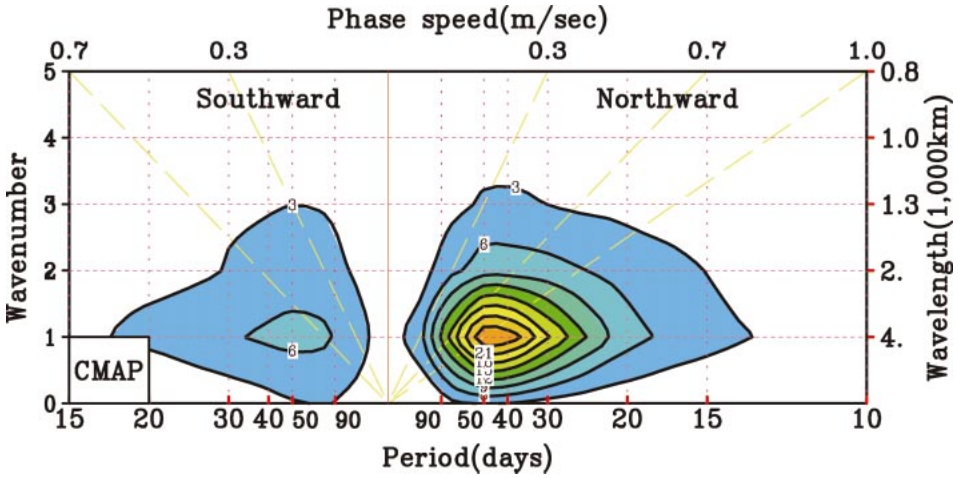

FIG. 1. The observed 10-yr (1991–2000) mean wavenumber-frequency spectra of pentad-mean rainfall from CMAP data (Xie and Arkin 1997); representing the northward- and southward-propagating disturbances in boreal summer over the Indian sector (between 65° and 95°E). Contour interval is 3 (mm day^{-1})^2.

During boreal summer, one dominant mode of BSISO in the Indian Ocean is the northward-propagating ISO (Yasunari 1980). The wavenumber-frequency analysis (Hayashi 1982; Teng and Wang 2003; Fu et al. 2003) is used to quantify the meridional propagating disturbances in the Indian sector. Figure 1 shows observed 10-yr mean rainfall variance associated with northward- and southward-propagating disturbances. The observed data are Climate Prediction Center (CPC) Merged Analysis of Precipitation (CMAP) pentad-mean rainfall from 1991 to 2000 (Xie and Arkin 1997). The northward-propagating disturbances, with a maximum spectrum about 24 (mm day^{-1})^2, apparently dominate their southward counterparts. The strongest northward disturbance has a period of 40–50 days and a meridional wavelength of about 40° with a phase speed of about 1 m s^{-1}, which is consistent with previous observational studies (Yasunari 1980).

The spatial–temporal characters of meridional-propagating ISOs are well reproduced by both coupled runs (DCPL, ICPL; Table 1). Figures 2a and 3a present the rainfall variance as functions of wavelengths and periods, respectively, for the DCPL and the ICPL. In both cases, the intensity of the northward-propagating ISO is significantly larger than their southward counterparts. The maximum spectra are 27 and 24 (mm day^{-1})^2, respectively, in the DCPL run and in the ICPL run with the dominant periods between 40 and 50 days.

The atmosphere-only run (DATM) forced with the truncated SST from the directly coupled run (DCPL) produces apparently weaker northward-propagating ISO compared to the corresponding coupled run (Figs. 2b,c). The maximum rainfall spectrum in this case is only about 18 (mm day^{-1})^2 (Fig. 2b), which is about 30% smaller than that in the DCPL run (Fig. 2c). In fact, the SST forcings to the atmospheric components of these two runs (DATM and DCPL) are almost the same except with a small truncation error in the DATM run. The resultant summer mean states between these two runs are very similar (see also Waliser et al. 1999). Therefore, the differences of BSISO between them are primarily due to air–sea coupling. Similar results are found for another atmosphere-only run (IATMi) forced with the daily mean SST from the indirectly coupled run (Figs. 3b,c). The only difference between the IATMi run and the ICPL run is the 1-day shift of initial conditions. For both the group of DCPL and DATM runs and the group of ICPL and IATMi runs, we found that northward-propagating ISOs are significantly stronger in the coupled runs than those in the atmosphere-only runs. This is consistent with our previous findings (Fu et al. 2003). However, the air–sea coupling does not significantly change the dominant period and propagating speed of the northward-propagating ISOs (Figs. 2, 3).

The systematically weaker northward-propagating ISOs in the atmosphere-only runs (cf. the coupled runs) may be due to the loss of coherent evolutions between atmospheric disturbances and underlying SST associated with BSISO. Figure 4 shows lag correlations between rainfall and SST for four experiments (DCPL, ICPL, DATM, and IATMi) with respect to the observations. Lag correlations are calculated with filtered rainfall and SST with only 20–70-day variability retained (Rui and Wang 1990). The observed rainfall and SST are, respectively, from the CMAP pentad-mean data (Xie and Arkin 1997) and Reynolds's weekly data (Reynolds 1988). The weekly SST has been interpolated into pentad data before extracting intraseasonal signals. Over both the Arabian Sea (Fig. 4a) and the Bay of Bengal (Fig. 4b), coupled solutions and atmosphere-only solutions are apparently separated from each other. The solutions of coupled runs are consistent with the observations (Sengupta et al. 2001; Vecchi

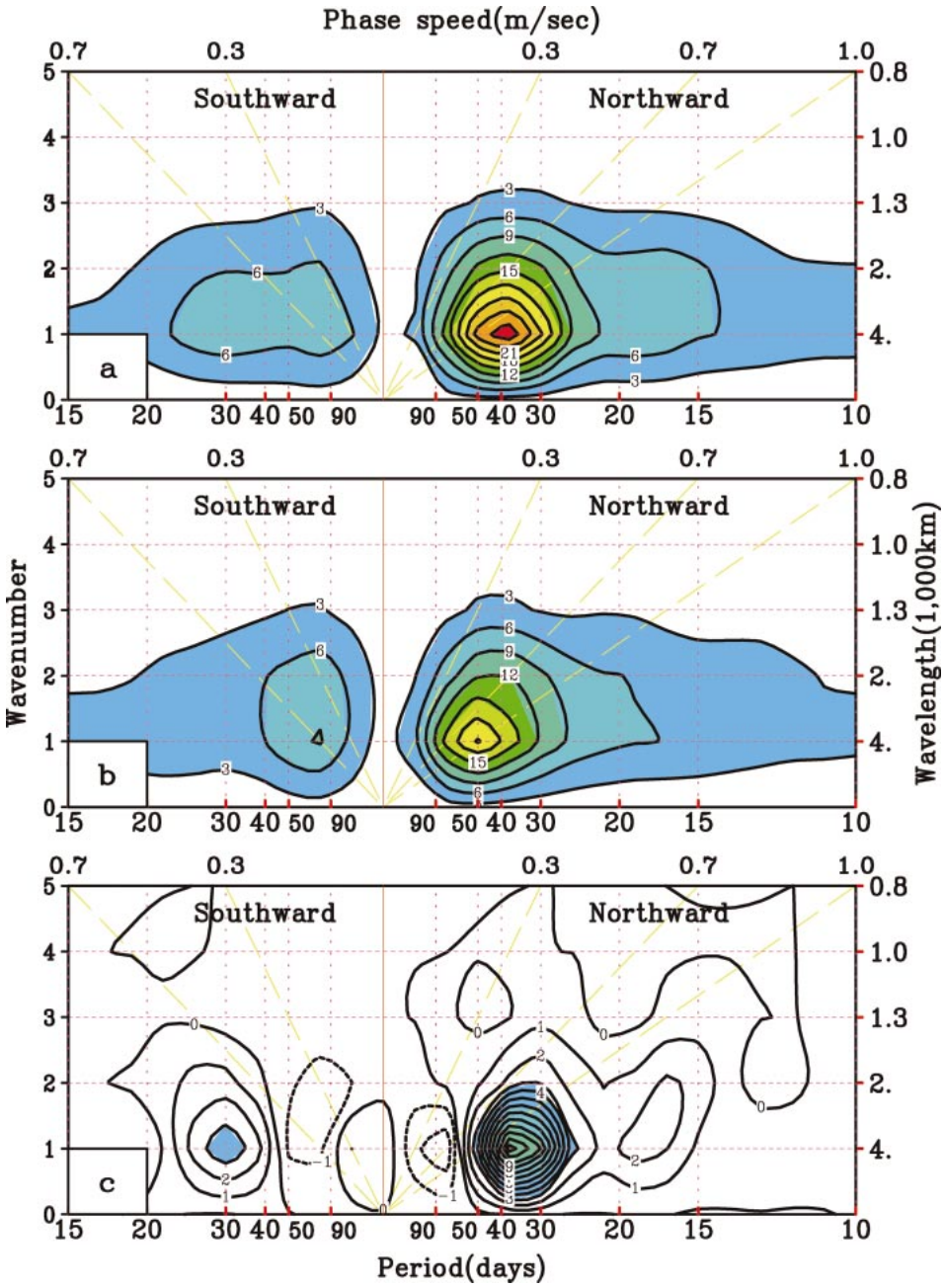

FIG. 2. The 10-yr mean wavenumber-frequency spectra of (a) the DCPL, (b) the DATM (Table 1), and the difference between (a) and (b). Contour interval is 3 for (a) and (b) but 1 (mm day^{-1})^2 for (c).

and Harrison 2002), whereas the solutions of atmosphere-only runs are different from the observations. In the coupled cases and the observations, positive (negative) SST systematically leads (lags) convection by two pentads with a correlation coefficient about 0.6 (-0.6). In the atmosphere-only cases, positive SST is almost in phase with rainfall with a smaller correlation coefficient between 0.2 and 0.4. The reduced correlation suggests that the convection associated with BSISO in the atmosphere-only system is less coherent with underlying SST compared to the coupled system (or the natural world).

Why is the convection of BSISO highly correlated with underlying SST in a coupled system? The basic reason is that the atmospheric disturbances associated with BSISO force coherent SST signals in the underlying oceanic mixed layer. These SST signals, on the other hand, significantly feed back to the atmospheric disturbances (Fu et al. 2003). Figure 5 shows the regressed patterns of rainfall, surface winds, surface heat

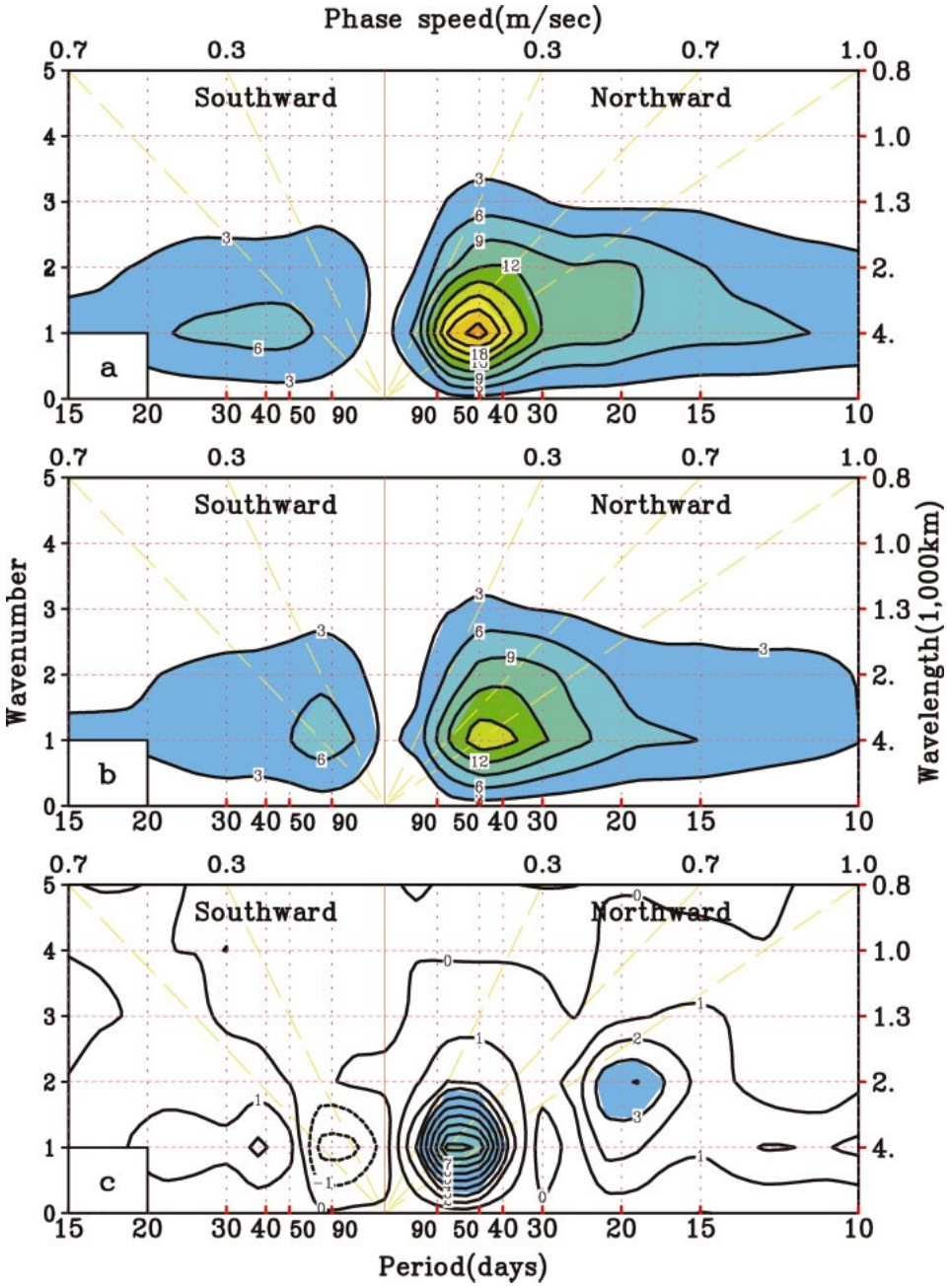

FIG. 3. The 10-yr mean wavenumber-frequency spectra of (a) the ICPL, (b) the IATMi (Table 1), and the difference between (a) and (b). Contour interval is 3 for (a) and (b) but 1 (mm day^{-1})^2 for (c).

fluxes, and sea surface temperature with 10-yr boreal summer output from the directly coupled run. All variables have been filtered to retain only variability with time scales of 20–70 days. The reference of regressions is the filtered pentad-mean rainfall at the equatorial western Indian Ocean. Once a convective disturbance appears at the Somali coast, an easterly anomaly is produced in the equatorial central-eastern Indian Ocean as a Kelvin wave response (Fig. 5a). The Rossby wave responses in off-equatorial regions are also easterly. Considering that mean surface flows are southeasterly in the southern Indian Ocean and southwesterly in the northern Indian Ocean, surface evaporation, therefore, will be increased in the southern side, but reduced in the northern side of the convection center (Fig. 5c). Downward solar radiation is reduced under the convection and significantly increased in the north and east of the convection (Fig. 5d) due to large mean cloudiness in these areas. The resultant net surface heat flux indicates a negative value nearby and south of the

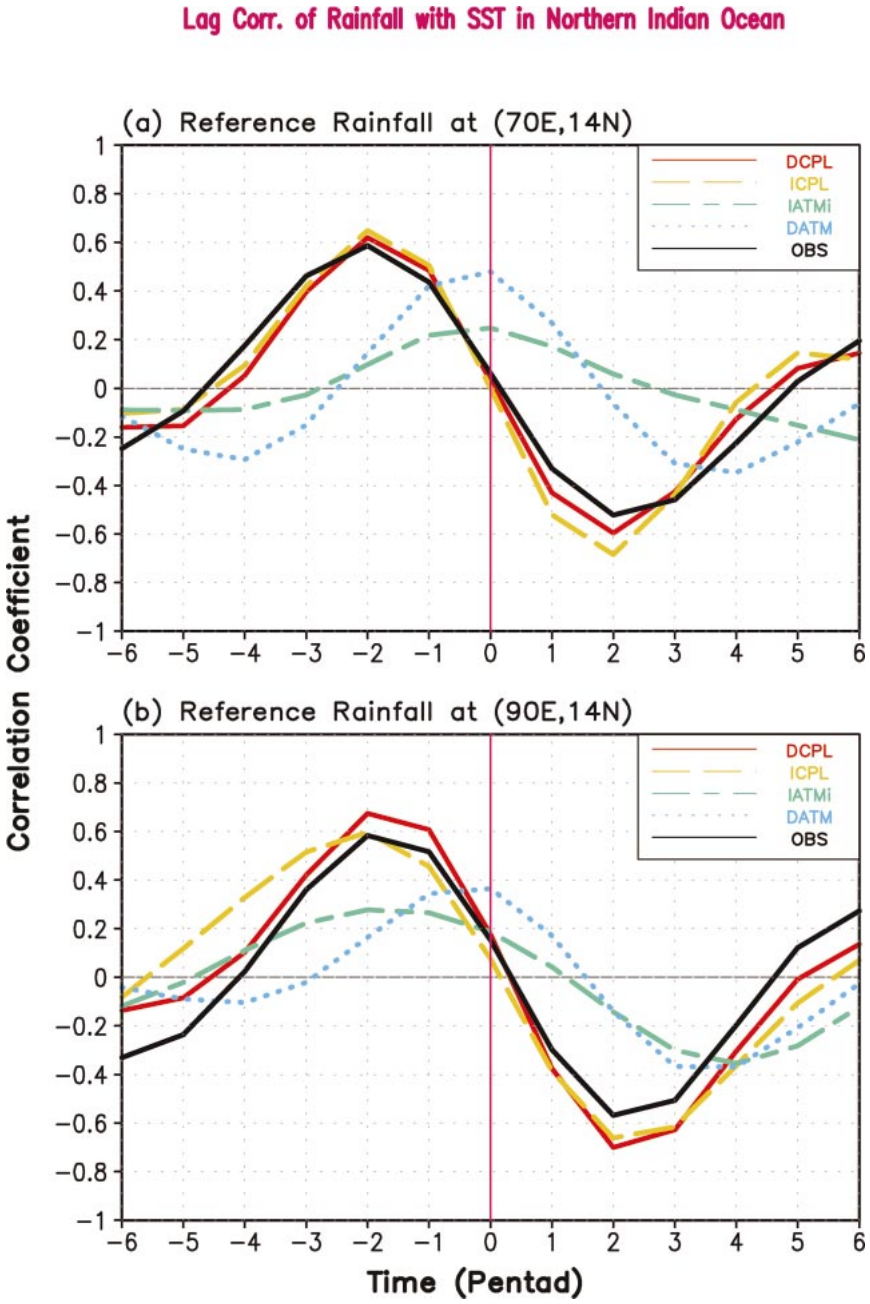

FIG. 4. The lag correlations of intraseasonal rainfall and local SST for the observations (obs) and the four experiments (Table 1) (a) over the Arabian Sea (14°N, 70°E) and (b) over the Bay of Bengal (14°N, 90°E).

equator, but positive north of the equator (Fig. 5b). Increased downward heat flux in the north of the convection warms up the sea surface there (Fig. 5b). The resultant positive SST helps the equatorial convection move northward. On the other hand, the cooling of sea surface underneath the convection tends to help it move away from its original position. With ECAHM4 AGCM, Fu et al. (2003) demonstrated that the intraseasonal SST fluctuations force considerable atmospheric responses. The systematically stronger northward-propagating ISOs in the coupled runs (cf. the atmospheric runs, particularly that forced with monthly mean SST) also substantiate that the intraseasonal SST positively feeds back to the atmospheric convection. Therefore, a coherent evolution among the convection, atmospheric circulations, and SST associated with BSISO is realized in this atmosphere–ocean coupled system.

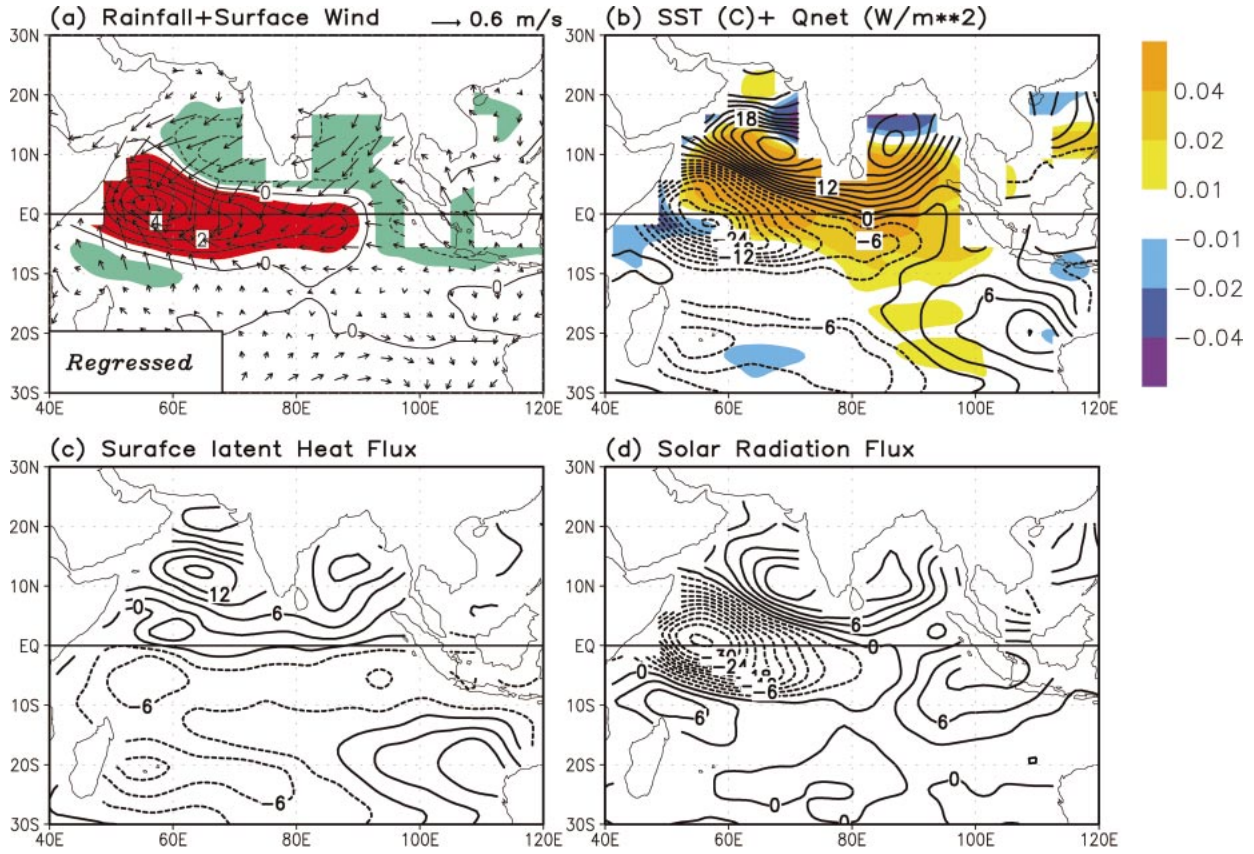

FIG. 5. Regressed (a) convective rainfall (contour interval: 1 mm day^{-1}) and surface winds, (b) net surface heat flux (CI: 3 W m^{-2}) and SST (°C, shaded), (c) surface latent heat flux (CI: 3 W m^{-2}) and (d) solar radiation (CI: 3 W m^{-2}) in the DCPL (Table 1).

4. Summary and discussion

The hybrid-coupled model, which combines ECHAM4 AGCM and the Wang–Li–Fu intermediate ocean model, well simulates the northward-propagating ISO in boreal summer over the Indian sector (Figs. 1, 2a, 3a, 4). Five sensitivity experiments (Table 1) with this hybrid-coupled model and its atmospheric component have been carried out to reveal the differences of intraseasonal solutions in the coupled model and the atmospheric model. When initial conditions and SST forcings are exactly the same for the coupled run and the atmospheric run (ICPL and IATM; Table 1), identical ISO solutions are found for both of them. Once there is a small amount of noise in the initial conditions or the SST forcings, the atmospheric model produces an ISO solution, which is quite different from that of the coupled model in at least two aspects. The intensity of northward-propagating ISO in the atmosphere-only model is about 30% weaker than that in the coupled model (Figs. 2, 3). The atmospheric model also cannot reproduce the phase relationship between SST and rainfall as seen in the coupled model and in the observations (Fig. 4). However, the air–sea coupling will not significantly change the dominant period and propagating speed of the northward-propagating ISO simulated in the atmospheric model. Better agreement between the coupled model and the observations suggests that, in nature, BSISO is a result of coherent interactions among convective disturbances, the associated atmospheric circulations, and the underlying sea surface temperature. We have also done the same analyses for the eastward-moving MJO in all above experiments (figure not shown). Similar results are found.

Therefore, to study ISO with atmosphere-only models may bear some limitations. First, atmosphere-only models may underestimate the intensity of ISO. Our previous study (Fu et al. 2003) showed that northward-propagating ISO in an atmosphere-only model forced with monthly mean SST (AMIP-type run) is about 50% weaker than that in the coupled run. With daily mean SST forcing, the intensity is still 30% weaker. It suggests that even forcing an atmospheric model with observed daily SST (subject to observational uncertainties) is unable to reproduce the full intensity of the observed ISO. This may explain why the northward-propagating ISOs in all 10 AGCMs participating in Climate Variability and Predictability (CLIVAR) Asian–Australian Monsoon AGCM Intercomparison Project are systematically weaker than the observations

(Waliser et al. 2002). Second, atmosphere-only approach cannot realistically capture the interaction between internal dynamics and underlying boundary conditions for intraseasonal oscillations. The coherent evolutions between convection and SST shown in the observations are only sustained by air–sea coupled models (Fig. 4). Further studies are needed to address these questions: Why do atmosphere-only models fail to sustain the quadrature phase relationship between convection and SST? How is that related to the structure and intensity of ISO? We also found that air–sea coupling does not significantly change the dominant period and the propagating speed of ISO in the ECHAM4 AGCM. This supports the atmosphere-only model as a good tool to study the internal dynamics of ISO. Air–sea interaction is one of many pieces in the puzzle of realistically simulating tropical intraseasonal oscillations. As suggested by Arakawa (2000), we should examine physical processes and calibrate our atmospheric model with all the important feedbacks involved. In the case of ISO, it would be better to test the sensitivity and calibration of cumulus parameterization, cloud–radiation interaction, and boundary layer process in an atmosphere–ocean coupled context.

Acknowledgments. This work was supported by NSF Grant ATM03-29531 and by the Frontier Research System for Global Change through its sponsorship of the IPRC. XF wishes to thank Dr. Julian P. McCreary for helpful discussions and Diane Henderson for editing the manuscript. Comments from two anonymous reviewers help improve the manuscript.

REFERENCES

Arakawa, A., 2000: Future development of general circulation models. *General Circulation Model Development: Past, Present and Future,* D. A. Randall, Ed., Academic Press, 721–773.

Bhat, G. S., and Coauthors, 2001: BOBMEX: The Bay of Bengal monsoon experiment. *Bull. Amer. Meteor. Soc.,* **82,** 2217–2243.

Bladé, I., and D. L. Hartmann, 1993: Tropical intraseasonal oscillations in a simple nonlinear model. *J. Atmos. Sci.,* **50,** 2922–2939.

Chen, T. C., R. Y. Tzeng, and M. C. Yen, 1988: Development and life cycle of the Indian monsoon: Effect of the 30–50 day oscillation. *Mon. Wea. Rev.,* **116,** 2183–2199.

Flatau, M., P. Flatau, P. Phoebus, and P. Niller, 1997: The feedback between equatorial convection and local radiative and evaporative processes: The implications for intraseasonal oscillations. *J. Atmos. Sci.,* **54,** 2373–2386.

Fu, X., and B. Wang, 2001: A coupled modeling study of the annual cycle of Pacific cold tongue. Part I: Simulation and sensitivity experiments. *J. Climate,* **14,** 765–779.

——, ——, and T. Li, 2002: Impacts of air–sea coupling on the simulation of the mean Asian summer monsoon in the ECHAM4 model. *Mon. Wea. Rev.,* **130,** 2889–2903.

——, ——, ——, and J. P. McCreary, 2003: Coupling between northward-propagating, intraseasonal oscillations and sea surface temperature in the Indian Ocean. *J. Atmos. Sci.,* **60,** 1733–1753.

Hayashi, Y., 1982: Space–time spectral analysis and its applications to atmospheric waves. *J. Meteor. Soc. Japan,* **60,** 156–171.

Hu, Q., and D. A. Randall, 1994: Low-frequency oscillations in radiative–convective systems. *J. Atmos. Sci.,* **51,** 1089–1099.

Inness, P. M., and J. M. Slingo, 2003: Simulation of the Madden–Julian oscillation in a coupled general circulation model. Part I: Comparison with observations and an atmosphere-only GCM. *J. Climate,* **16,** 345–364.

Kemball-Cook, S., B. Wang, and X. Fu, 2002: Simulation of the intraseasonal oscillation in the ECHAM4 model: The impact of coupling with an ocean model. *J. Atmos. Sci.,* **59,** 1433–1453.

Lau, K. M., and P. H. Chan, 1986: Aspects of the 40–50 day oscillation during the northern summer as inferred from outgoing longwave radiation. *Mon. Wea. Rev.,* **114,** 1354–1367.

——, and L. Peng, 1987: Origin of low frequency (intraseasonal) oscillations in the tropical atmosphere. Part I: The basic theory. *J. Atmos. Sci.,* **44,** 950–972.

Lawrence, D. M., and P. J. Webster, 2002: The boreal summer intraseasonal oscillation: Relationship between northward and eastward movement of convection. *J. Atmos. Sci.,* **59,** 1593–1606.

Liebmann, B., H. H. Hendon, and J. D. Glick, 1994: The relationship between tropical cyclones of the western Pacific and Indian Oceans and the Madden–Julian Oscillation. *J. Meteor. Soc. Japan,* **72,** 401–411.

Mo, K. C., 2000: Intraseasonal modulation of summer precipitation over North America. *Mon. Wea. Rev.,* **128,** 1490–1505.

Raymond, D. J., 2001: A new model of the Madden–Julian oscillation. *J. Atmos. Sci.,* **58,** 2807–2819.

Reynolds, R. W., 1988: A real-time global sea surface temperature analysis. *J. Climate,* **1,** 75–86.

Roeckner, E., and Coauthors, 1996: The atmospheric general circulation model ECHAM4: Model description and simulation of present-day climate. Max-Planck-Institute for Meteorology Rep. 218, 90 pp.

Rui, H., and B. Wang, 1990: Development characteristics and dynamic structure of tropical intraseasonal convection anomalies. *J. Atmos. Sci.,* **47,** 357–379.

Sengupta, D., B. N. Goswami, and R. Senan, 2001: Coherent intraseasonal oscillations of ocean and atmosphere during the Asian summer monsoon. *Geophys. Res. Lett.,* **20,** 4127–4130.

Slingo, J. M., and Coauthors, 1996: Intraseasonal oscillations in 15 atmospheric general circulation models: Results from an AMIP diagnostic subproject. *Climate Dyn.,* **12,** 325–357.

Teng, H., and B. Wang, 2003: Interannual variations of the boreal summer intraseasonal oscillation in the Asian–Pacific region. *J. Climate,* **16,** 3572–3584.

Vecchi, G., and D. E. Harrison, 2002: Monsoon breaks and subseasonal sea surface temperature variability in the Bay of Bengal. *J. Climate,* **15,** 1485–1493.

Waliser, D. E., K. M. Lau, and J. H. Kim, 1999: The influence of coupled sea surface temperatures on the Madden–Julian oscillation: A model perturbation experiment. *J. Atmos. Sci.,* **56,** 333–358.

——, and Coauthors, 2003: AGCM simulations of intraseasonal variability associated with the Asian summer monsoon. *Climate Dyn.,* **21,** 423–446.

Wang, B., 1988: Dynamics of tropical low frequency waves: An analysis of moist Kelvin waves. *J. Atmos. Sci.,* **45,** 2051–2065.

——, and X. Xie, 1997: A model for the boreal summer intraseasonal oscillation. *J. Atmos. Sci.,* **54,** 72–86.

——, and X. Xu, 1997: Northern Hemisphere summer monsoon singularities and climatological intraseasonal oscillation. *J. Climate,* **10,** 1071–1085.

——, and X. Xie, 1998: Coupled modes of the warm pool climate system. Part I: The role of air–sea interaction in maintaining Madden–Julian Oscillation. *J. Climate,* **11,** 2116–2135.

——, T. Li, and P. Chang, 1995: An intermediate model of the tropical Pacific Ocean. *J. Phys. Oceanogr.,* **25,** 2051–2065.

Webster, P. J., and Coauthors, 2002: The JASMINE Pilot Study. *Bull. Amer. Meteor. Soc.,* **83,** 1603–1629.

Weller, R. A., and S. P. Anderson, 1996: Surface meteorology and

air–sea fluxes in the western equatorial Pacific warm pool during the TOGA COARE. *J. Climate*, **9,** 1959–1990.

Wu, M. L., S. Schubert, I. S. Kang, and D. E. Waliser, 2002: Forced and free intraseasonal variability over the south Asian monsoon region simulated by 10 AGCMs. *J. Climate*, **15,** 2862–2880.

Xie, P., and P. A. Arkin, 1997: Global precipitation: A 17-year monthly analysis based on gauge observations, satellite estimates, and numerical model outputs. *Bull. Amer. Meteor. Soc.*, **78,** 2539–2558.

Yasunari, T., 1980: A quasi-stationary appearance of 30 to 40 day period in the cloudiness fluctuations during the summer monsoon over India. *J. Meteor. Soc. Japan*, **58,** 225–229.